

# Chapter 1

## General Information About Piezoelectric Sensors

### 1.1 Short Historical Essay

The history of piezoelectricity development totals more than 120 years. In 1880, Pierre and Jacques Curie found that under pressure some materials develop surface electrical charges. Subsequently, this effect was named the “piezoeffect”; electricity caused by mechanical pressure was called “piezoelectricity”, and materials (quartz, turmalin, segnet salt, etc.) in which there is this phenomenon were called “piezoelectric” [1].

In 1881, G. Lippmann foretold that electric voltage enclosed in piezoelectric material would cause mechanical pressure and elastic deformations [2]. This was proven experimentally by P. Curie and J. Curie [3]. The phenomenon has been named the “return piezoeffect.” The word “piezo”, borrowed from Greek, means “I press.”

Practical application of the piezoelectric effect began in 1917 when a French mathematician and physicist, Paul Langevin, suggested using an ultrasonic echo ranging device for detection of underwater objects. In this device (a projector and receiver of ultrasonic signals), quartz plates were built between steel overlays, thus lowering the resonant frequency of the transducer [4]. Initially, an ultrasonic locator was used by Langevin in a quality echo sounder. Further improvement led to the creation of modern ultrasonic echo sounders and various underwater detection devices (including those attached to submarines).

Soon after Langevin’s invention, the first piezoelectric microphones, phones, sound pickups, devices for sound recordings, devices for vibration measurements, forces and accelerations, etc. were created.

Piezoelectric plates and pivots were to be used as the stabilizing elements; frequency of electronic high-frequency generators followed as an important stage in the application history of piezoelectricity. Applications were based on a strong frequency piezoelement dependence on electrical impedance near the mechanical resonance, as investigated by W. Cady in 1922 [5].

In 1925, G. Pierse used an acoustic interferometer for ultrasound speed measurement in gases [6]. It was the first piezoelectric plate application for measuring the acoustic properties of a substance.

This opened the possibility of detecting internal defects in solid materials by using ultrasonic waves; this was an important application of piezoelectricity for practical purposes. C. Sokolov received a USSR copyright for the invention of the first ultrasonic flaw detector (non-destructive testing) [7].

Development of measurement methods concerning speed and absorption of ultrasound, based on light diffraction effects on ultrasonic waves, followed. Piezoelectric transducers were used by P. Debye and F. Sears [8] in 1932, for hypersonic research of substances, as well as by R. Lucas and P. Biquard [9]. Work involving this method was used for speed measurement and measuring ultrasound absorption in liquids and solids, which began in 1936.

In 1944, at the USSR's Lebedev Physical Institute, B.M. Wool and I.P. Goldman first developed a method of synthesizing piezoceramic titanium barium ( $\text{BaTiO}_3$ ) [10, 11]. Titanium, a barium preliminary, was polarized in a strong electric field; soon, piezoceramic electroacoustic transducers were developed [12, 13].

The scope of piezoelectric transducers extended rapidly after 1945. A variety of new areas, such as ultrasonic delay lines, ultrasonic medical therapy and diagnostics, level gauges, devices for continuous industrial control of physical and chemical substance properties, and other devices with wide applications were found for piezoelectric transducers. At the same time, more effective electroacoustic transducers became available.

Development of the theory and practice of piezoelectric devices is connected also with: U. Mason [12, 14, 15], L. Bergman [16], W. Cady [5, 17], R. Thurston [18], G.V. Katts [19], M. Onoe [20], H. Tiersten [21], N.N. Andreev [22, 23], A.A. Harkevich [24], I.P. Goljamina [25], V. Domarkas and R. Kazys [26, 27], V.V. Malov [28], A.N. Kutsenko [29], L.J. Gutin [30], N.A. Shulga, A.M. Bolkisev [31], V.V. Lavrinenko [32], I.A. Glozman [33], S.I. Pugachev [34], O.P. Kramarov [35], A.F. Ulitko [36], I.G. Minaev [37], A.I. Trofimov [38], A.E. Kolesnikov [39], M.V. Korolev [35], I.N. Yermolov [40], R.G. Dzhangupov [41], V.M. Pluzhnikov [42], P.O. Gribovskiy [43], P.G. Pozdnyakov [44], V.M. Sharapov [45], and many others.

## 1.2 Determination and Classification of Piezoelectric Sensors

This book is devoted to piezoelectric transducers; therefore, it is necessary to agree on terminology. Transducers will transform one physical size or one type of information to another physical size or another type of information. Therefore, a sensor can be called a pressure transducer in an electrical signal, or a transducer of electric voltage from one level of voltage to another level (electric transformer).

In technical language there is also the concept “sensor”, which is equivalent to the concept “primary transducer.”

In this book, there will be information about piezoelectric sensors (transducers of physical sizes to an electric signal) and also about other piezoelectric transducers.

Piezoelectric transducers contain crystals or structures which electrosize under the influence of mechanical pressure (a “straight-line piezoeffect”) and deformed structures in an electric field called “return piezoeffect.”

A feature of the piezoeffect is sign sensitivity, when a charged sign changes or when compression is replaced; this sign stretching and changing produces a directional field change [46, 47].

Many crystal substances possess piezoelectric properties: quartz, turmalin, niobium, lithium, segnet salt, etc. Artificial polycrystalline materials are also produced which polarize in the electrical field (piezoelectric ceramics), e.g., titanium barium, titanium lead, zirconium lead, etc. [48].

Piezoelectric transducers are used for measuring mechanical parameters (effort, pressure, acceleration, weight, angular speed, moments, deformations, etc.), thermal sizes (temperature, expense, vacuum, electric parameters, etc.) and for structure control, gas concentration, humidity, and micro weights [28]. For accuracy, these devices in many cases surpass transducers based on other physical resolution principles.

Piezoelectric sensors can be divided into two large classes depending on their basic physical effects:

- Sensors in the first class use a straight-line piezoeffect. They are used for measuring linear and vibrating accelerations, dynamic and quasistatic pressure and efforts, as well as parameters of sound and ultrasonic fields, etc. [45].
- A second but no less extensive class of sensors concerns the so-called resonant piezotransducers [28, 38, 49], which use the return piezoeffect. They are resonant sensors from piezoelectric resonators, and they can also produce straight-line piezoeffects. (These are resonant piezoelectric transformer sensors.) In addition, other physical effects can be used, e.g., tensosensitivity, acoustosensitivity, thermosensitivity, etc., allow utilization for measurement of static and/or dynamic pressure and efforts, linear and vibrating accelerations, concentration of gas substances, viscosity, inclination corners, etc. [41, 45].

The largest class of piezoceramic sensors can be classified as follows:

1. Sensors on applied materials:
  - Monocrystal materials (quartz, niobium lithium, etc.)
  - Polycrystalline materials (piezoceramic)
2. By fluctuations:
  - On the linear size
  - On the radial
  - On curving
  - On torsion (rotation?)
  - On the shift (shear modes)
  - On surface acoustic waves
  - On a combined configuration

3. By the physical effects:

- Thermosensitivity
- Tensosensitivity
- Acoustosensitivity
- Gyrosensitivity
- Contact (using contact rigidity and the actual contact area, etc.)
- Domain dissipative, etc.

4. By the quantity of the piezoelements:

- Monoelement
- Bimorph (symmetric or asymmetric)
- Threemorph, etc.

5. By destination:

- For measurement of dynamic pressure and efforts
- For measurement of linear accelerations
- For measurement of vibration parameters
- For measurement of static pressure and efforts
- For measurement of blow parameters
- For measurement of sound pressure
- For humidity measurement
- For viscosity measurement
- For hydroacoustics
- For gyroscopes
- For gas analyzers
- For temperature measurement
- For contact rigidity measurement
- For measurement of the actual area of contact
- For magnetic size measurement
- For optics measurement
- For micromoving measurement
- For dust concentration measurement
- In ultrasonic technology
- In electroacoustics
- In automatics devices
- In communication
- In electronic techniques and radio engineering
- In medicine:
  - For ultrasonic tomographs
  - For pulse measurement
  - For tone measurement by Korotkov
  - For urology
  - For ophthalmology

And others.

### 1.3 Properties and Descriptions of Piezomaterials

The piezoeffect's physical nature can be shown with quartz, the most common piezoelectric crystal [46, 47]. Figure 1.1a shows the basic crystal quartz cell structure. The cell as a whole is electrically neutral; however, it is possible to allocate three directions which pass through the center and two different uniter ion polars. The polars are called electric axes or axes  $X$ , with polarization vectors  $\mathbf{P}_1$ ,  $\mathbf{P}_2$ , and  $\mathbf{P}_3$ .

If force  $\mathbf{F}_x$  in regular intervals is distributed on the side, a perpendicular axis  $X$  results; the broken electric neutrality of the elementary cell is enclosed in a quartz crystal along the axis. Shown in Fig. 1.1b, the unformed cell ( $\mathbf{P}_2$  and  $\mathbf{P}_3$  on axis  $X$  vector projections) decreases with compression or increases with vector  $\mathbf{P}_1$  stretching. As a result, the polarization vector appears equally effective, and there are corresponding polarizing charges on the sides. Compression signs are shown in Fig. 1.1b. It is easy to see that cell deformation does not influence the electric condition along axis  $Y$ . Here the vector projection sum is equal to zero, for  $\mathbf{P}_{2Y} = \mathbf{P}_{3Y}$ .

Polarizing charge formation on the sides and perpendicular axes  $X$ , with force on axis  $X$ , is called the *longitudinal piezoeffect*.

Mechanical pressure enclosed along one of the  $Y$  axes is called *mechanical axes*. The geometrical sum of vectors  $\mathbf{P}_2$  and  $\mathbf{P}_3$  on a  $Y$  axis projection is equal to zero. When the  $Y$  axis piezoelement sides are perpendicular, charges are not

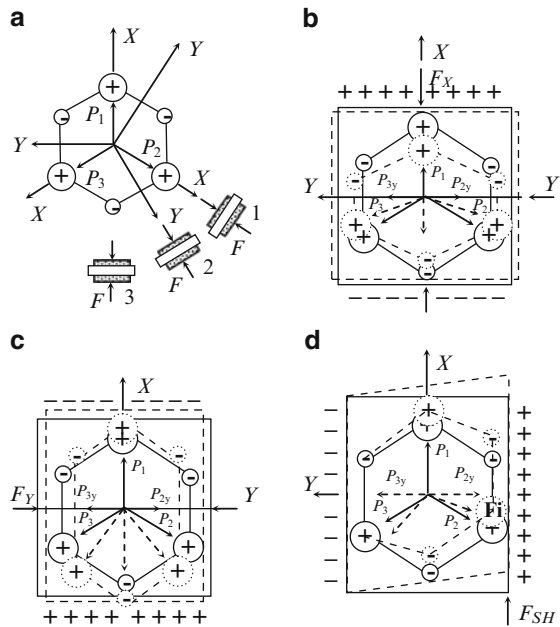


**Fig. 1.1** Elementary quartz cell crystal structure

formed. However, vectors  $\mathbf{P}_2$  and  $\mathbf{P}_3$  on the  $X$  axis projection sum are not equal to vector  $\mathbf{P}_1$ . Hence, with piezoelement compression, as represented in Fig. 1.1c, the sum exceeds  $\mathbf{P}_1$ . As a result, the bottom side forms positive charges and the top side forms negative charges. The formation of side charges, perpendicular to the loaded sides, is called *transverse*.

When uniformly loaded from different directions, as for example in hydrostatic compression, the quartz crystal remains electrically neutral. When loading  $Z$  axis perpendicular to axes  $X$  and  $Y$  with a crystal optical axis, the quartz crystal remains electrically neutral. Mechanical pressure shift deformation is shown in Fig. 1.1d. When the geometrical sum of vectors  $\mathbf{P}_2$  and  $\mathbf{P}_3$  on  $X$  axis projections is equal to vector  $\mathbf{P}_1$  directed on  $X$  axes and on the sides of perpendicular  $X$  axes, the charge does not increase. However, when vectors  $\mathbf{P}_2$  and  $\mathbf{P}_3$  on the  $Y$  axis are not equal projections and the  $Y$  axis sides are perpendicular, there is a charge.

When considering the physical nature, the piezoeffect shows that intense quartz charges can rise between three side steams. The polarizing quartz charge is a vector that can be described by three components. The intense condition is characterized as a second-rank tensor with nine components.

A piezoelectric module defining charge dependences from an intense condition is a third-rank tensor; it is defined by 27 components.

However, tensor mechanical pressure contains only six independent components, which are designated as  $\sigma_{11} = \sigma_1$ ,  $\sigma_{22} = \sigma_2$ ,  $\sigma_{33} = \sigma_3$ ,  $\sigma_{23} = \sigma_4$ ,  $\sigma_{13} = \sigma_5$ , and  $\sigma_{12} = \sigma_6$ . It passes to a simplified piezo-module form presented in a table containing 18 components:

$$d_{ij} = \begin{bmatrix} d_{11}d_{12}d_{13}d_{14}d_{15}d_{16} \\ d_{21}d_{22}d_{23}d_{24}d_{25}d_{26} \\ d_{31}d_{32}d_{33}d_{34}d_{35}d_{36} \end{bmatrix}. \quad (1.1)$$

With the piezo-module table, it is possible to calculate charge density on all three sides after any pressure [46].

The basic advantages of quartz are great hardness, insolubility in water, stability when exposed to some acids, small thermal expansion, extremely good mechanical quality ( $10^5$ – $10^6$ ), and parameter stability ( $10^{-3}$ – $10^{-5}\%$ ).

However, the electromechanical communication coefficient of quartz is approximately ten times greater, and the piezo-modules are less than the corresponding piezoceramic parameters. In addition, quartz has low dielectric permeability and its own plate capacity; therefore, the shunting capacity of the cable and entrance chains in the measuring devices considerably reduces transducer sensitivity. The important constraining factor in pressure quartz transducer utilization is its high cost and production difficulties [50, 51].

The most utilized piezoelectric materials are piezoceramics, which appeared only in the early 1960s when industrial synthesized natural piezoelectric materials like quartz were mastered. With high-sensitivity segnet salt, turmalin and others, the mechanical durability was raised by temperature stability. Now in domestic and foreign literature, many publications speak about piezoceramic element applications, so they have been introduced to the industry [41].

Piezoceramics possess many advantages.

Piezoceramic elements are rather economical, and they possess high radiating firmness in various active environments. Only hydre fluoric acid is capable of having a destroying effect on piezoceramics; thus, piezoceramic devices can be utilized in many difficult chemical situations.

When compared with quartz, piezoceramic material has a low Curie  $T_K$  point value. For quartz this  $T_K$  value =  $570^\circ\text{C}$ , while for piezoceramics with titanium barium the  $T_K$  value is  $100\text{--}200^\circ\text{C}$ . There are high-temperature piezoceramic materials with Curie points within quartz matter. Hence, some piezoceramic-made elements of IITC (PZT) do not lose working capacity at temperatures of  $300\text{--}400^\circ\text{C}$ , e.g., IITC-21 has  $T_K = 400^\circ\text{C}$ . With cobalt, they are able to maintain a temperature of  $700^\circ\text{C}$  and more.

The wide temperature ranges allow piezoceramic sensor usage from 400 to  $270^\circ\text{C}$ . Moreover, special transducers can be used for pressure measurement in internal combustion engine cylinders, where temperatures fluctuate from normal to  $+1,600^\circ\text{C}$ .

Piezoceramic sensors with decimals increase the measurement range usage.

Piezoceramic sensors have high resolution; as an illustration, if a 100T locomotive is put on piezoelectric scales and the measurement range on the panel of the charging amplifier is switched, it is possible to measure the additional weight of a pencil put on the locomotive's footboard.

Piezoelectric transducers can maintain high pressures, measuring pressures to 10,000 bar. They have great rigidity; that is especially important when manufacturing measurement dynamometers in a wide range of frequencies.

## 1.4 Transducer Research Methods

The piezoelectric material “deformation” theory developed from a joint electro-dynamics and mechanics project; recently, this emerged as an independent field of study [31].

Anisotropy of piezoelectric material's physical and mathematical properties and electromagnetic field interrelations with mechanical movements complicate deformation and durability description processes. Considerable attention has been given to creating and developing quantitative analyses.

Basic linear theory electroelasticity parities [31] consisted of equations describing the mechanical piezoeffect. These equations follow preservation laws and necessary geometrical communications, and are fair for any linear environment. Maxwell equations describe the environmental electrical phenomena. Communication between two types of equation variables is defined by physical parities – the piezoeffect equations. Electric induction vectors, an intense electric field, and symmetric mechanical tensor pressure cause deformations. Linear communication factors are complex. Introduction of the complex factors makes it possible to consider dissipation in piezoelectric material cyclic deformation.

The piezoelectric body equation-defining system consists of 22 differential equations. Regional electroelasticity problems are possible only in rare instances for elementary areas. It is necessary to be satisfied with an approached decision [31].

Effective construction remedies of the approached decision vary. Different formulations make it necessary to find a corresponding variation principle with a stationary value.

To understand piezoelectric body proceeding processes, one-dimensional problems for bodies with a degenerative geometry, e.g., cores, thin disks and plates, rings, and infinite cylinders, have essential value. The fluctuations can be described by scalar equations when exact decisions are needed.

An alternative approach is piezoelectric material replacement by an equivalent electrical scheme, and then making subsequent calculations under the electric chains theory [19]. This approach is natural with coordination questions and with a general electric chain analysis, which is part of the piezoelectric material equivalent circuit. But questions of mechanical and electrical durability or optimum design remain in relation to electric chain frameworks.

One-dimensional problems have a special practical value. First, one-dimensional fluctuations are found in many concrete devices; second, complex physical parity factors are experimental on one-dimensional measurements.

Extensive problems exist with regard to axial symmetry piezoelectric body fluctuations. Mathematical axial symmetry fluctuations, spatial from a physical point, are usually described by two-dimensional equations [31].

Theoretical automatic control methods are also widely applied to transducer analysis [26, 27]. The most exact results can be derived by experimentation.

## 1.5 Piezoceramic Material and Element Parameters

Parameters of piezoceramic materials are normalized [52] and defined [53]. The basic characteristics in piezoceramic materials are:

1. Electromechanical communication ( $K_p$ )
2. Relative dielectric permeability (constant or permittivity) ( $\epsilon_{33}^T/\epsilon_0$ )
3. Specific volume electric resistance ( $\rho_v$ )
4. Density ( $\rho$ )
5. Water absorption ( $W$ )
6. Piezo-modules in a dynamic mode ( $d_{31}$ ,  $d_{33}$ )
7. Piezo-modules in a static mode ( $d_{31}$ )
8. Young's modulus ( $Y_{31}^Y$ )
9. Speed of a sound ( $v_i^j$ )
10. Good mechanical quality ( $Q_M$ )
11. Relative frequency deviation in the range of working temperatures from the frequency measured at the adjustment temperature ( $\delta f_\Theta/f_r$ )



12. Corner of dielectric losses tangent in weak electric fields ( $\operatorname{tg} \delta$ )
13. Electrical durability ( $E_{np}$ )
14. Temperature of Curie ( $T_C$ )
15. Mechanical durability limit with static compression ( $\sigma_{\text{compr}}$ )
16. Mechanical durability limit with static bend ( $\sigma_b$ )
17. Mechanical durability limit with static stretching ( $\sigma_{\text{str}}$ )

Additional characteristics:

18. Piezo-module in a dynamic mode
19. Piezo-module in quasistatic mode
20. Mechanical durability limit with static stretching

Additional characteristics would be defined when necessary by manufacturers.

## 1.6 Determining Piezoceramic Element Parameters

### 1.6.1 Defining the Electromechanical Communication Coefficient

The electromechanical communication  $K_p$  coefficient is calculated by the formula:

$$K_p = \sqrt{\frac{\eta^2 - \sigma^2}{2(1 + \sigma)}} \left( 1 - \frac{f_r^2}{f_a^2} \right), \quad (1.2)$$

where  $\eta$ , the least positive root of the frequency equation;  $\sigma$ , Poisson's coefficient;  $f_r$ , resonant frequency, Hz;  $f_a$ , antiresonant frequency, Hz.

### 1.6.2 Phase Measurement of Resonant $f_r$ and Antiresonant $f_a$ Frequencies of Radial and Longitudinal Fluctuations

The installation diagram used for measurement is shown in Fig. 1.2.

### 1.6.3 Measurement of Resonant Frequency $f_r$

Established in nests XS4 holder  $E$  with sample  $BQ$ . From generator  $G$  on a two-port network  $R1$  input (socket XS1) gives a signal of such value that on an input of the sample (socket XS2) the voltage was  $200 \pm 20$  mV. Voltage supervised with the help of millivoltmeter  $PV1$ . Socket  $XP8$  connects with loading resistor  $R3^*$  ( $R3^* =$

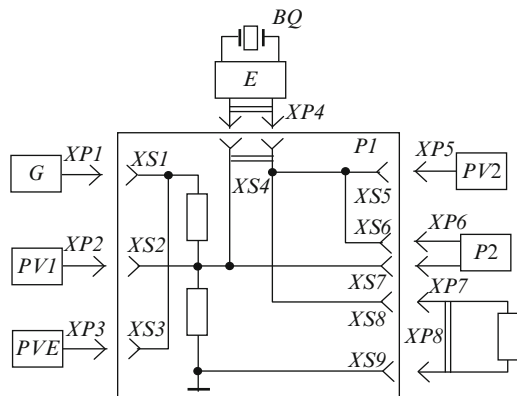


**Fig. 1.2** Installation for measuring  $f_r$  and  $f_a$ :  $G$ , generator of signals;  $PV1$ ,  $PV2$ , millivoltmeters;  $PF$ , electronic frequency meter;  $XP1$ - $XP8$ ,  $XS1$ - $XS9$ , sockets;  $BQ$ , test piece;  $E$ , test piece holder;  $P1$ , passive two-port network ( $R1 = 68 \text{ ohm}$ ,  $R2 = 7.6 \text{ ohm}$ )  $R1 = (8 - 10)R2$ ,  $R1 + R2 = R_{\text{out a gen}}$ ,  $R3^* = 1 \text{ ohm}/100 \text{ kohm}$ ; Connecting mark cables PK-75-4-11 – PK-75-4-16 no more than 0.5 m in length

2 kohm – for samples  $16 \times 3 \times 3 \text{ mm}$  and  $R3^* = 2 \text{ kohm}$  – for samples  $\varnothing 10 \times 1 \text{ mm}$ , resistance values are specified roughly). Smoothly changing generator  $G$  frequency achieves the maximum deviation of an arrow millivoltmeter  $PV2$ , thus voltage on the exit sample should be within 10–15 mV.

If voltage on millivoltmeter  $PV2$  is distinct from that specified above, it is necessary to pick up the resistance value of loading resistor  $R3^*$ . Then, changing the frequency of generator  $G$  achieves phase zero under the indication phase meter  $P2$ . If signal value for the phase meter is not enough, an amplifier with a minimum phase shift in a range of frequencies and its further account is supposed to be used. Thus, it is necessary to calibrate a new phase meter  $P2$ . In phase zero there is a corresponding resonant frequency  $f_r$  which measure by a frequency meter  $PF$ .

A tuning phase meter is not supposed to be for measuring resonant frequency  $f_r$ .

### 1.6.4 Measurement of Antiresonant Frequency $f_r$

To socket  $XP8$  connect loading resistor  $R3^*$  ( $R3^* = 50 \text{ kohm}$  – for samples  $16 \times 3 \times 3 \text{ mm}$  and  $R3^* = 50 \text{ ohm}$  – for samples  $\varnothing 10 \times 1 \text{ mm}$  of resistance value are specified roughly). Smoothly changing generator  $G$  frequency achieves the minimum deviation of an arrow millivoltmeter  $PV2$ , thus voltage should be within 1–3 mV.

If voltage on millivoltmeter  $PV2$  is different from that specified above, it is necessary to pick up the resistance value of the loading resistor  $R3^*$ . Then, change the generator  $G$  frequency achieves phase zero under the indication phase meter  $P2$ .

If a signal value for the phase meter is not enough, the amplifier takes into account the phase shift. Thus, it is necessary to calibrate a new phase meter *P2*.

When measuring antiresonant frequency, it is necessary to use the holder with a minimum electric capacity. If antiresonant frequency displacement, at the expense of the holder's electric capacity, is more than 5% from the static electric capacity, it can be defined by the formula:

$$\frac{\Delta f_a}{f_a} = \frac{f_a - f_r}{f_r - f_a R_0^2} \frac{C_{\text{hol}} - 0.05 C_0}{C_0}, \quad (1.3)$$

where  $f_a$ , antiresonant frequency, Hz;  $f_r$ , resonant frequency, Hz;  $C_{\text{hol}}$ , electric capacity of the holder, pF;  $C_0$ , electric static capacity, pF;  $R_0 = R_r/|X_{C_0}| = 2\pi f_r C_0 R_r$ , test piece resistance on the resonant to frequency of jet resistance of the test piece, ohm;  $|X_{C_0}|$ , jet resistance of electric static capacity;  $R_r$ , resistance of the sample on the resonant frequency, calculated with definition of good mechanical quality, ohm.

### 1.6.5 *Best (Amplitude?) Method of Measuring Resonant $f_r$ and Antiresonant $f_a$ Frequencies*

Measurements using Fig. 1.2 without a phase meter. The frequency  $f_r$  value corresponds to the maximum deviation millivoltmeter *PV2*; and the minimum deviation millivoltmeter *PV2* corresponds to the frequency  $f_a$ . Frequency value is measured by a frequency meter *PF*.

### 1.6.6 *Measurement of Frequency in the First Overtone $f_{01}$*

Measurement of frequency in the first overtone  $f_{01}$  radial and longitudinal fluctuations on an earlier specified installation (Fig. 1.2) without applying a phase meter was performed in the following order: to socket *XP8*, connect loading resistor  $R3^*$  ( $R3^* = 2 \text{ kohm}$ , for samples  $16 \times 3 \times 3 \text{ mm}$  and  $R3^* = 1 \text{ ohm}$  for samples  $\varnothing 10 \times 1 \text{ mm}$ , values of resistance are specified roughly). Smoothly changing generator *G* frequency to increase from  $f_r$  will achieve the maximum deviation of an arrow on millivoltmeter *PV2*. Thus, voltage should be within 5–15 mV.

If voltage on millivoltmeter *PV2* is different from that specified above, it is necessary to pick up resistance values by loading resistor  $R3^*$ . The maximum deviation of the arrow millivoltmeter *PV2* corresponds to the frequency of the first overtone  $f_{01}$ , and is measured by a frequency meter *PF*.

### 1.6.7 Definition of Poisson's Coefficient $\sigma$

Poisson's coefficient  $\sigma$  depends on the value of factor  $\beta$  chosen from Table 1.1.

The coefficient is calculated by the formula:

$$\beta = \frac{f_{01}}{f_r}, \quad (1.4)$$

where  $f_{01}$ , frequency of the first overtone, Hz;  $f_r$ , the resonant frequency is defined by a peak method, Hz.

### 1.6.8 Definition of the Least Positive Root of the Frequency Equation $\eta$

The least positive root of the frequency equation  $\eta$  depends on the value of Poisson's coefficient  $\sigma$  chosen from Table 1.2.

### 1.6.9 Relative Dielectric Permeability (Constant, Permittivity?) $\epsilon_{33}^T/\epsilon_0$

Relative dielectric permeability of a material is calculated by the formula:

$$\epsilon_{33}^T/\epsilon_0 = \frac{11.3C_0b}{S_e}, \quad (1.5)$$

where  $C_0$ , static electrical capacity of the test piece, pF;  $b$ , thickness of the sample, cm;  $S_e$ , surface area of an electrode, cm<sup>2</sup>.

**Table 1.1**

$\beta$	2.6746	2.6670	2.6559	2.6529	2.6448	2.6375	2.6304	2.6237	2.6173
$\sigma$	0.24	0.25	0.26	0.27	0.28	0.29	0.30	0.31	0.32
$\beta$	2.6097	2.6040	2.5963	2.5897	2.5832	2.5775	2.5705	2.5642	
$\sigma$	0.33	0.34	0.35	0.36	0.37	0.38	0.39	0.40	

**Table 1.2**

$\sigma$	0.24	0.25	0.26	0.27	0.28	0.29	0.30	0.31	0.32
$\eta$	2.0112	2.0179	2.0238	2.0300	2.0362	2.0425	2.0488	2.0551	2.0612
$\sigma$	0.33	0.34	0.35	0.36	0.37	0.38	0.39	0.40	0.41
$\eta$	2.0673	2.0735	2.0795	2.0855	2.0915	2.0974	2.1041	2.1109	2.1150
$\sigma$	0.42	0.43	0.44	0.45	0.46	0.47	0.48	0.49	0.50
$\eta$	2.1208	2.1266	2.1323	2.1380	2.1436	2.1492	2.1548	2.1604	2.1659

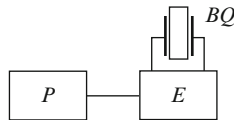


**Fig. 1.3** Installation for measurement  $C_0.P$ , universal bridge;  $BQ$ , test piece;  $E$ , test piece holder

In the formula, actual linear size values for each sample should be substituted (Fig. 1.3).

### 1.6.10 Specific Volume Electric Resistance $\rho_v$

Specific volume electric resistance  $\rho_v$  (Gohm  $\cdot$  cm), the defined test sample, measuring resistance of its isolation with constant voltage no more than 100 V. Relative measurement error should remain under  $\pm 20\%$ . Resistance readout measured for 1 minute from giving the measured pressure.

Value of the specific volume electrical resistance  $\rho_v$  is calculated by the formula:

$$\rho_v = R \frac{S_e}{b}, \quad (1.6)$$

where  $R$ , resistance of isolation, Gohm;  $S_e$ , area of an electrode surface,  $\text{cm}^2$ ;  $b$ , thickness of the test piece, cm.

### 1.6.11 Defining Piezo-modules $d_{31}$ and $d_{33}$ in a Dynamic Mode

Piezo-module  $d_{31}$  (Kl/N) in a dynamic mode is calculated using the formula:

$$d_{31} = \frac{0.19 \times 10^{-5} K_p}{f_r} \frac{2}{D} \sqrt{\frac{\varepsilon_{33}^T}{\varepsilon_0} \frac{1}{\rho}}, \quad (1.7)$$

where  $K_p$ , electromechanical communication coefficient;  $D$ , disk diameter, cm;  $f_r$ , resonant frequency of the radial fluctuations, Hz;  $\varepsilon_{33}^T/\varepsilon_0$ , relative dielectric permeability;  $\rho$ , density,  $\text{cm}^3$ .

Piezo-module  $d_{33}$  (C/N) in a dynamic mode is defined by measuring resonant  $f_r$  and antiresonant  $f_a$  frequencies of longitudinal fluctuations using the formula:

$$d_{33} = \frac{0.24 \times 10^{-5} \pi}{f_r f_a l} \sqrt{\frac{(f_a^2 - f_r^2) \varepsilon_{33}^T}{2 \rho \varepsilon_0}}, \quad (1.8)$$

where  $f_r$ ,  $f_a$ , resonant and antiresonant frequencies, Hz;  $\varepsilon_{33}^T/\varepsilon_0$ , relative dielectric permeability;  $l$ , test piece length, cm;  $\rho$ , density,  $\text{g}/\text{cm}^3$ .

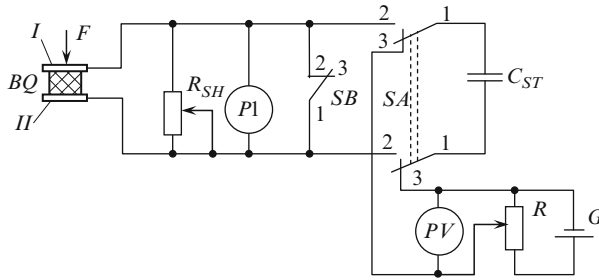


**Fig. 1.4** Installation for measurement  $d_{33}$ : 1, 2, 3 – switch and button positions;  $I$  – mobile electrode to which  $F$  is loaded;  $BQ$  – test piece;  $II$  – motionless electrode  $R_{SH}$  – shunting resistance for adjusting galvanometer sensitivity;  $P1$  – galvanometer ballistic mirror;  $SB$  – button closing galvanometer chain;  $SA$  – dual switch on two positions;  $C_{ST}$  – standard condenser (steals up experimentally, with approximate electric capacity 1,000–5,000 pF);  $PV$  – direct current voltmeter, a class 0.5 that limits measurements to 30 In;  $R$  – potentiometer, which helps establish necessary voltage on standard condenser;  $G$  – source of direct current voltage to 30 V

### 1.6.12 Piezo-module $d_{33}$ in a Static Mode

Piezo-module  $d_{33}$  in a static mode is defined by measuring the charge value on the electrodes of the test piece, when removing the loading enclosed on the polarization axis. The installation block diagram is shown in Fig. 1.4. Electrodes should be located perpendicularly to the loading direction.

Piezo-module  $d_{33}$  is calculated by the formula:

$$d_{33} = \frac{Q}{F} = K\alpha, \quad (1.9)$$

where  $Q$ , charge emergent on electrodes, C;  $F$ , force enclosed in the test piece, H;  $K$ , correction coefficient from  $F$ ;  $\alpha$ , mirror ballistic galvanometer light index deviation at measurement, mm.

The sample's emergent charge under force is measured by a galvanometer.

Force exerted on the sample by a special adaptation gives a chance to sharply remove enclosed mechanical stress.

The wire capacitance, connecting the sample with the installation, should be no more than 10 pF from installation to the galvanometer, and no more than 110 pF. Relative error of the Piezo-module  $d_{33}$  should be no more than  $\pm 10\%$ .

### 1.6.13 Young's Modulus $Y_{31}^Y$

Young's modulus  $Y_{31}^Y$  (Pa), in a dynamic mode, is defined using the formula:

$$Y_{31}^Y = \frac{0.4\pi^2}{\eta^2} f_r^2 \frac{D^2}{4} \rho (1 - \sigma^2), \quad (1.10)$$

where  $f_r$ , resonant frequency of radial fluctuations, Hz;  $D$ , disk diameter, cm;  $\rho$ , density, g/cm<sup>3</sup>;  $\sigma$ , Poisson's coefficient;  $\eta$ , least positive root of frequency equation chosen from Table 1.2, depending on value  $\sigma$ .

### 1.6.14 Speed of Sound $v_3^D$

The speed of sound  $v_3^D$  (km/s) is calculated by the following formulas:

- for a bar-shaped test sample

$$v_3^D = 2 \times 10^{-2} f_a l, \quad (1.11)$$

where  $f_a$ , antiresonant frequency of longitudinal fluctuations, Hz;  $l$ , length of the test sample, m.

- for a disk-shaped test sample

$$v_1^E = \frac{f_r \pi D}{\eta} \sqrt{1 - \sigma^2}, \quad (1.12)$$

where  $f_r$ , resonant frequency of radial fluctuations, Hz;  $D$ , diameter of the test sample, m;  $\sigma$ , Poisson's coefficient was chosen from Table 1.2;  $\eta$ , least positive frequency equation root was chosen from Table 1.2 depending on value  $\sigma$ .

### 1.6.15 Good Mechanical Quality $Q_m$

Good mechanical quality  $Q_m$  was calculated by formulas

$$Q_m = \frac{f_a^2 \times 10^{12}}{2\pi R_r C_0 f_r (f_a^2 - f_r^2)}, \quad (1.13)$$

where  $R_r = R_l[(U_{in}/U_{out}) - 1]$ , resonator resistance on the resonant frequency calculated with a margin of error  $\pm 10\%$ , ohm;  $R_l = R_3$ , loading resistance is included in the block diagram Fig. 1.1 at measurement  $f_r$ , ohm;  $U_{in}$ , device input voltage, measured millivoltmeter PV1, V;  $U_{out}$ , device exit voltage (resonant frequency) measured on millivoltmeter PV2, V;  $C_0$ , test piece static electric capacity measured on frequency of 1,000 Hz, pF.

### 1.6.16 Definition of Curie Point Temperature $T_C$

The Curie point temperature  $T_C$  in piezoceramic material is the temperature when the dielectric permeability's (constant, permittivity?) maximum size is observed, calculated on the sample's measured value of static capacity.

Temperatures of Curie point (C) samples are defined in a heat chamber. For a valid temperature value, ten samples were received for measurement and an average temperature value of the Curie point was accepted.

Measurement of static capacity begins at  $298 \pm 10 \text{ K}$  ( $25 \pm 10^\circ\text{C}$ ). Then static capacity, in the temperature ranges, is measured when temperatures rise. Heat the sample with a speed that is no more than  $5 \text{ K}$  ( $5^\circ\text{C}$ ) per minute, a  $30\text{--}50 \text{ K}$  ( $30\text{--}50^\circ\text{C}$ ) below Curie point temperature on the concrete mark. After that, temperatures increase at a speed less than  $2 \text{ K}$  ( $2^\circ\text{C}$ ) in a minute. During the process, it is necessary to measure the capacity of all tested samples; the heat chamber temperature should be supported with a margin error no more  $\pm 2 \text{ K}$  ( $\pm 2^\circ\text{C}$ ).

After establishing the set temperature of the static capacity  $C_0$ , directly control the chamber by means of a universal bridge or other device which will provide measurement on a frequency of  $1,000 \pm 200 \text{ Hz}$ , with a margin error of no more  $\pm 1\%$ .

## 1.7 Piezoceramic Materials

Piezoelectric ceramic materials (PCMs) present ferroelectric connections or firm solutions received by synthesizing various oxides and salts (Table 1.3) [43,53,54].

Modern PCM is made with solid solutions such as lead zirconate titanate (PZT, in Russian IITC), which has been modified by various components and additives. PCM based on titanate barium, titanate bismuth, titanate lead, and niobate lead is also produced. The basic properties in PCM, as revealed on standard ceramic test samples, are:

- High values of dielectric permeability (constant, permittivity?)
- Presence of spontaneous polarization in separate areas (domains)
- Presence of hysteresis loops in dependences, e.g., polarization-electric fields and deformation-electric fields
- Growth of dielectric permeability (constant, permittivity?) when temperatures rise
- Presence of Curie temperature point without curve dependence of dielectric permeability (constant, permittivity?) temperatures above ferroelectric properties
- Residual polarization occurrence and double cake-like electric layer on the surface after constant electric field influence, causing display possibilities by the piezoelectric effect body (transforming mechanical energy into electrical energy and/or vice versa)

Depending on their basic purpose, PCMs are subdivided as follows:

1. “Ferro-soft” PCM can be applied to high-sensitivity transducer manufacturing, working without rigid requirements on parameter stability to influence destabilizing factors (raised temperatures and electric or mechanical fields).

General purpose PCMs for materials IITC-19 (PZT-5A) and IITC-19 (IIT): IITC-19 (IIT) is the updated IITC-19 with raised values of piezoelectric modules ( $d_{ik}$ ). This increase is reached at the expense of replacement of raw



components zirconium oxide and titanium oxide on specially developed highly active raw materials – titanium zirconium.

PCM has a lowered dielectric permeability(constant, permittivity?) and high reception sensitivity ( $g_{ik}$ ). The material IITC-36 ) is usually used in hot-extrusion blocks and is intended, mainly, for manufacturing transducers with ultrasonic delay lines.

PCM has raised values of dielectric permeability(constant, permittivity?) and piezo-module (HIITC-2). These materials are intended for use in telephone devices with hypersensitivity.

2. “Ferro- hard” PCM is applied to transducers working in a reception environment and/or radiation where strong electric fields and/or mechanical pressure influence the conditions. They utilize IITC-23, IITCCT-3(IIT), and IITBC-7 materials. Materials IITC-23 and IITCCT-3(IIT) are well proven in ignition and hydroacoustic piezoelement systems. It is possible to recommend IITCCT-3(IIT) and IITBC-7 for manufacturing piezotransformers and ultrasonic radiators (projectors?) of a raised capacity.
3. PCM, for frequency-selective devices, is applied to piezoelement manufacturing because it possesses characteristics that can cope with raised temperatures and time stability frequency. Frequency-selective devices are for volume and surface acoustic waves (SAW).

Materials for frequency-selective devices for volume waves of planar fluctuations are applied when creating filters on discrete piezoelements; the materials used include IITC-38, IITC-39, and IITC-40.

Materials for frequency-selective devices with volume waves of a compression-stretching fluctuation (thickness) are in subgroups IITC-35 and IITC-35Y.

In hot compacting blocks, IITC-35Y is issued.

Materials for frequency-selective devices with volume waves of a shift thickness fluctuation are represented by a subgroup material IITC-35. Materials in subgroups 3.2 and 3.3 are used to create monolithic filters for frequency-modulated signals on frequencies to 10 MHz.

Materials for frequency-selective devices for superficial acoustic waves include IITC-33, produced in hot compacting blocks. It is applied by setting filters to 40 MHz frequencies.

4. High-temperature PCM is used for piezoelement manufacturing in devices that work at temperatures at not less than 250°C, which includes the materials IITC-21, IITC-26, THaB-1, and THB-1. For piezoelements with working temperatures of 250–750°C, the material IITC-26 was developed. For increased temperature stability, piezo-module ( $d_{33}$ ), THaB-1, IITC-26M, and THaB-1M have been developed.
5. Electro-optical materials are used for manufacturing active elements for light modulation, including protective devices and digital indicators. This group includes the materials IITCJI-A, IITCJI-B, and IITCJI-B. Elements from a material IITCJI-A, with residual polarization, are used in the linear EO effect (Pockel's effect). They are characterized also by record-breaking high

piezoelectric and pyroelectrical parameters. Elements from TSTSL-IN are used in light modulation; the devices work in a square law EO effect (the Kerr effect) with various temperature intervals.

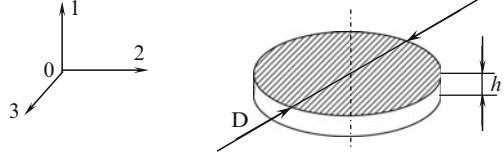
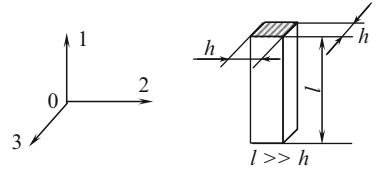
Basic characteristics of some described piezoelectric ceramic materials are presented in Table 1.3. Additional information about piezoelectric materials can be found on Open Society “ELPA” (Zelenograd, Russia) at <http://www.aha.ru/~elpa/> and Open Society “Aurora” (Volgograd, Russia) at <http://www.avrora.vlink.ru>.

Transducer parameters are defined by problems which they solve.

## 1.8 Formulas for the Calculation of Piezoceramic Material Descriptions

### 1.8.1 Piezoceramic Disk (Fig. 1.5)

$$\begin{aligned}
 K_{31} &= -\sqrt{\frac{\frac{\pi}{2} \frac{f_{a1}}{f_{r1}}}{\frac{\pi}{2} \frac{f_{a1}}{f_{r1}} - \operatorname{tg}\left(\frac{\pi}{2} \frac{f_{a1}}{f_{r1}}\right)}}, \\
 K_p &= |K_{31}| \sqrt{\frac{2}{1-\sigma}} = \sqrt{\frac{2}{1-\sigma} \frac{\frac{\pi}{2} \frac{f_{a1}}{f_{r1}}}{\frac{\pi}{2} \frac{f_{a1}}{f_{r1}} - \operatorname{tg}\left(\frac{\pi}{2} \frac{f_{a1}}{f_{r1}}\right)}}, \\
 S_{11}^E &= \frac{\chi^2}{\pi^2(1-\sigma^2)\rho} \frac{1}{(Df_{a1})^2}; \quad S_{12}^E = -S_{11}^E \sigma = -\frac{\sigma \chi^2}{\pi^2(1-\sigma^2)\rho} \frac{1}{(Df_{a1})^2}; \\
 \frac{\varepsilon_{33}^T}{\varepsilon_0} &= \frac{11.3 \times 10^{10} h \times 4}{\pi D^2} C_0; \quad C_{01} = C_{ad1} \frac{f_a' - f_r}{f_{a1} - f_{a1}'}; \quad \frac{\varepsilon_{33}^S}{\varepsilon_0} = (1 - K_p^2) \frac{\varepsilon_{33}^T}{\varepsilon_0}; \\
 d_{31} &= |K_{31}| \sqrt{S_{11}^E \varepsilon_{33}^T} = \frac{\chi}{\pi D f_{a1}} \sqrt{\frac{\frac{\pi}{2} \frac{f_{a1}}{f_{r1}}}{\frac{\pi}{2} \frac{f_{a1}}{f_{r1}} - \operatorname{tg}\left(\frac{\pi}{2} \frac{f_{a1}}{f_{r1}}\right)} \frac{\varepsilon_{33}^T}{(1-\sigma^2)\rho}}; \\
 g_{31} &= \frac{d_{31}}{\varepsilon_{33}^T} = \frac{\chi}{\pi D f_{a1}} \sqrt{\frac{\frac{\pi}{2} \frac{f_{a1}}{f_{r1}}}{\frac{\pi}{2} \frac{f_{a1}}{f_{r1}} - \operatorname{tg}\left(\frac{\pi}{2} \frac{f_{a1}}{f_{r1}}\right)} \frac{1}{(1-\sigma^2)\rho \varepsilon_{33}^T}}; \\
 S_{11}^D &= S_{11}^E - d_{31} g_{31} = \frac{\chi^2}{\pi^2 \rho (1-\sigma^2) (Df_{a1})^2} \left[ 1 - \frac{\frac{\pi}{2} \frac{f_{a1}}{f_{r1}}}{\frac{\pi}{2} \frac{f_{a1}}{f_{r1}} - \operatorname{tg}\left(\frac{\pi}{2} \frac{f_{a1}}{f_{r1}}\right)} \right].
 \end{aligned}$$

**Fig. 1.5** Piezoceramic disk**Fig. 1.6** Piezoceramic bar

### 1.8.2 Piezoceramic Bar (Fig. 1.6)

$$K_{33} = \sqrt{\frac{\pi}{2} \frac{f_{r2}}{f_{a2}} \text{ctg} \left( \frac{\pi}{2} \frac{f_{r2}}{f_{a2}} \right)}; \quad S_{33}^E = \frac{1}{4l^2 \rho f_{a2}^2} \frac{1}{1 - \frac{\pi}{2} \frac{f_{r2}}{f_{a2}} \text{ctg} \left( \frac{\pi}{2} \frac{f_{r2}}{f_{a2}} \right)};$$

$$S_{33}^D = S_{33}^E (1 - K_{33}^2) = \frac{1}{4l^2 \rho f_{a2}^2}; \quad \frac{\varepsilon_{33}^T}{\varepsilon_0} = \frac{11.3 \times 10^{10} l}{h^2} C_{02};$$

$$C_{02} = C_{ad2} \frac{f_{a2}' - f_{r2}}{f_{a2} - f_{a2}'}; \quad \frac{\varepsilon_{33}^S}{\varepsilon_0} = (1 - K_{33}^2) \frac{\varepsilon_{33}^T}{\varepsilon_0};$$

$$d_{33} = K_{33} \sqrt{S_{33}^E \varepsilon_{33}^T} = \frac{1}{2l f_{a2}} \sqrt{\frac{\varepsilon_{33}^T}{\rho} \frac{\frac{\pi}{2} \frac{f_{r2}}{f_{a2}} \text{ctg} \left( \frac{\pi}{2} \frac{f_{r2}}{f_{a2}} \right)}{1 - \frac{\pi}{2} \frac{f_{r2}}{f_{a2}} \text{ctg} \left( \frac{\pi}{2} \frac{f_{r2}}{f_{a2}} \right)}};$$

$$g_{33} = \frac{d_{33}}{\varepsilon_{33}^T} = \frac{1}{2l f_{a2}} \sqrt{\frac{1}{\varepsilon_{33}^T \rho} \frac{\frac{\pi}{2} \frac{f_{r2}}{f_{a2}} \text{ctg} \left( \frac{\pi}{2} \frac{f_{r2}}{f_{a2}} \right)}{1 - \frac{\pi}{2} \frac{f_{r2}}{f_{a2}} \text{ctg} \left( \frac{\pi}{2} \frac{f_{r2}}{f_{a2}} \right)}}.$$

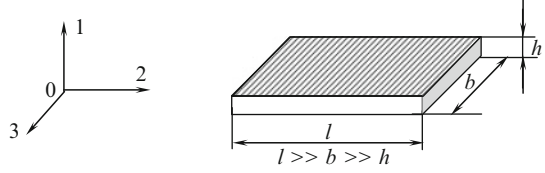
### 1.8.3 Piezoceramic Rectangular Plate (Fig. 1.7)

$$K_{15} = \sqrt{\frac{\pi}{2} \frac{f_{r3}}{f_{a3}} \text{ctg} \left( \frac{\pi}{2} \frac{f_{r3}}{f_{a3}} \right)}; \quad C_{44}^D = 4\rho h^2 f_{a3}^2; \quad C_{55}^D = C_{44}^D = 4\rho h^2 f_{a3}^2;$$

$$S_{44}^D = \frac{1}{C_{44}^D} = \frac{1}{4\rho h^2 f_{a3}^2}; \quad S_{55}^D = S_{44}^D = \frac{1}{4\rho h^2 f_{a3}^2};$$

$$C_{44}^E = C_{44}^D (1 - K_{15}^2) = 4\rho h^2 f_{a3}^2 \left[ 1 - \frac{\pi}{2} \frac{f_{r3}}{f_{a3}} \text{ctg} \left( \frac{\pi}{2} \frac{f_{r3}}{f_{a3}} \right) \right];$$

**Fig. 1.7** Piezoceramic rectangular plate



$$C_{55}^E = C_{44}^E = 4\rho h^2 f_{a3}^2 \left[ 1 - \frac{\pi}{2} \frac{f_{r3}}{f_{a3}} \operatorname{ctg} \left( \frac{\pi}{2} \frac{f_{r3}}{f_{a3}} \right) \right];$$

$$S_{44}^E = \frac{1}{C_{44}^E} = \frac{1}{4\rho h^2 f_{a3}^2 \left[ 1 - \frac{\pi}{2} \frac{f_{r3}}{f_{a3}} \operatorname{ctg} \left( \frac{\pi}{2} \frac{f_{r3}}{f_{a3}} \right) \right]};$$

$$S_{55}^E = S_{44}^E = \frac{1}{4\rho h^2 f_{a3}^2 \left[ 1 - \frac{\pi}{2} \frac{f_{r3}}{f_{a3}} \operatorname{ctg} \left( \frac{\pi}{2} \frac{f_{r3}}{f_{a3}} \right) \right]};$$

$$\frac{\varepsilon_{11}^T}{\varepsilon_0} = \frac{11.3 \times 10^{10} h}{lh} C_{03}; \quad C_{03} = C_{ad3} \frac{f'_{a3} - f_{r3}}{f_{a3} - f'_{a3}}; \quad \frac{\varepsilon_{11}^S}{\varepsilon_0} = (1 - K_{15}^2) \frac{\varepsilon_{11}^T}{\varepsilon_0};$$

$$d_{15} = K_{15} \sqrt{S_{44}^E \varepsilon_{11}^T} = \frac{1}{2hf_{a3}^2} \sqrt{\frac{\frac{\pi}{2} \frac{f_{r3}}{f_{a3}} \operatorname{ctg} \left( \frac{\pi}{2} \frac{f_{r3}}{f_{a3}} \right) \varepsilon_{11}^T}{\left[ 1 - \frac{\pi}{2} \frac{f_{r2}}{f_{a2}} \operatorname{ctg} \left( \frac{\pi}{2} \frac{f_{r2}}{f_{a2}} \right) \right] \rho}};$$

$$g_{15} = \frac{d_{15}}{\varepsilon_{11}^T} = \frac{1}{2hf_{a3}} \sqrt{\frac{\frac{\pi}{2} \frac{f_{r3}}{f_{a3}} \operatorname{ctg} \left( \frac{\pi}{2} \frac{f_{r3}}{f_{a3}} \right)}{\left[ 1 - \frac{\pi}{2} \frac{f_{r3}}{f_{a3}} \operatorname{ctg} \left( \frac{\pi}{2} \frac{f_{r3}}{f_{a3}} \right) \right] \varepsilon_{11}^T \rho}};$$

$$A = \frac{-2K_{33}K_p \pm \sqrt{4K_{33}^2K_p^2 - 4(K_{15}^2K_p^2 - K_{15}^2 - K_p^2)(K_{15}^2 - K_{15}^2K_p^2 - K_{33}^2)}}{2(K_{15}^2K_p^2 - K_{15}^2 - K_p^2)};$$

$$S_{13}^E = \frac{A}{\sqrt{2}} \sqrt{S_{33}^E(S_{11}^E + S_{12}^E)}; \quad S_{13}^D = S_{13}^E - d_{31}d_{33} \frac{1}{\varepsilon_{33}^T};$$

$$C_{11}^E = \frac{S_{11}^E S_{33}^E - (S_{13}^E)^2}{(S_{11}^E - S_{12}^E) [S_{33}^E(S_{11}^E + S_{12}^E) - 2(S_{13}^E)^2]};$$

$$C_{12}^E = \frac{-S_{12}^E S_{33}^E + (S_{13}^E)^2}{(S_{11}^E - S_{12}^E) [S_{33}^E(S_{11}^E + S_{12}^E) - 2(S_{13}^E)^2]};$$

$$C_{13}^E = \frac{-S_{13}^E}{S_{33}^E(S_{11}^E + S_{12}^E) - 2(S_{13}^E)^2}; \quad C_{33}^E = \frac{S_{11}^E + S_{12}^E}{S_{33}^E(S_{11}^E + S_{12}^E) - 2(S_{13}^E)^2};$$

$$\begin{aligned}
C_{11}^D &= \frac{S_{11}^D S_{33}^D - (S_{13}^D)^2}{(S_{11}^D - S_{12}^D) [S_{33}^D (S_{11}^D + S_{12}^D) - 2(S_{13}^D)^2]}; \\
C_{12}^D &= \frac{-S_{12}^D S_{33}^D + (S_{13}^D)^2}{(S_{11}^D - S_{12}^D) [S_{33}^D (S_{11}^D + S_{12}^D) - 2(S_{13}^D)^2]}; \\
C_{13}^D &= \frac{-S_{13}^D}{S_{33}^D (S_{11}^D + S_{12}^D) - 2(S_{13}^D)^2}; \quad C_{33}^D = \frac{S_{11}^D + S_{12}^D}{S_{33}^D (S_{11}^D + S_{12}^D) - 2(S_{13}^D)^2}; \\
h_{15} &= g_{15} C_{44}^D = \frac{d_{15}}{\varepsilon_{11}^T} C_{44}^D; \quad h_{31} = \frac{d_{31}(C_{11}^D + C_{12}^D) + d_{33} C_{13}^D}{\varepsilon_{33}^T}; \\
h_{33} &= \frac{2d_{31} C_{31}^D + d_{33} C_{33}^D}{\varepsilon_{33}^T}; \quad e_{15} = h_{15} \varepsilon_{11}^S = d_{15} C_{44}^E; \\
e_{31} &= h_{31} \varepsilon_{33}^S = d_{15}(C_{11}^E + C_{12}^E) + d_{33} C_{13}^E; \quad e_{33} = h_{33} \varepsilon_{33}^S = 2d_{31} C_{13}^E + d_{33} C_{33}^E; \\
C_{66}^D &= \frac{1}{2}(C_{11}^D + C_{12}^D); \quad C_{66}^E = C_{66}^D; \quad S_{66}^D = \frac{1}{C_{66}^D}; \quad S_{66}^E = S_{66}^D;
\end{aligned}$$

where  $h$ , thickness of the test piece, mm;  $D$ , diameter of the test piece, mm;  $l$ , length of the test piece, mm;  $C_{ad1,2,3}$ , additional capacity  $F$  included in parallel to the sample for definition of dielectric permeability on antiresonant frequency;  $\rho$ , density, kg/sm<sup>2</sup>;  $\varepsilon_0$ , dielectric permeability is equal  $8.85 \times 10^{-12}$ ,  $\Phi/\text{M}$ ;  $f_{r1}$ ,  $f_{r2}$ ,  $f_{r3}$ , resonance frequency in the corresponding test piece, Hz;  $f_{a1}$ ,  $f_{a2}$ ,  $f_{a3}$ , antiresonance frequency of the corresponding test piece, Hz;  $f'_{a1}$ ,  $f'_{a2}$ ,  $f'_{a3}$ , antiresonance displacement frequency in additional capacity, Hz;  $g_{31}$ ,  $g_{33}$ ,  $g_{15}$ , piezoelectric constants, Vm/N;  $d_{31}$ ,  $d_{33}$ ,  $d_{15}$ , piezoelectric constants, Kl/N;  $h_{31}$ ,  $h_{33}$ ,  $h_{15}$ , piezoelectric deformation factors, V/m;  $e_{31}$ ,  $e_{33}$ ,  $e_{15}$ , piezoelectric constants;  $C_{11}$ ,  $C_{12}$ ,  $C_{13}$ ,  $C_{33}$ ,  $C_{44}$ ,  $C_{55}$ ,  $C_{66}$ , elastic constants with indexes  $E$  and  $D$ , H/M<sup>2</sup>;  $S_{11}$ ,  $S_{12}$ ,  $S_{13}$ ,  $S_{33}$ ,  $S_{44}$ ,  $S_{55}$ ,  $S_{66}$ , elastic constants with indexes  $E$  and  $D$ , m<sup>2</sup>/H;  $\chi$ , a constant equalling 2.069.

## 1.9 Sensor [Physical Size] Descriptions

Basic sensor characteristics are a range of measurements, sensitivity, a threshold of reaction (sensitivity), errors, time of indication establishment, and reliability [46, 55].

1. *Range of measurements* – measured size values in which we normalize supposed errors. This range is subject to measurement limits, greatest and least values of the measurement range.
2. *Sensitivity*  $S$  – change relationship between an output sensor  $\Delta Y$  signal to the change which caused it on the measured size  $\Delta X$ :  $S = \Delta Y / \Delta X$ .

3. *Errors* – with series graduation of the same sensors it appears that the characteristics differ from each other. In the measuring transducer passport, some average characteristics “nominal” are observed. Differences between the “nominal passport” and the real sensor characteristics are considered its “error.”
4. *Reliability* – transducer’s ability to keep characteristics in certain limits during the established time interval, under set operation conditions.

## References

1. J. Curie, P. Curie, Développement, par pression, de l’électricité polaire dans les cristaux hémiedres a faces inclinées. *Compt. Rend.* **91**, 294–295 (1880)
2. G. Lippmann, Principe de la conversation de l’électricité. *Ann. de Chim. et de Phys.* **24**, 145–178 (1881)
3. J. Curie, P. Curie, Contractions et dilatations produits par des tensions électriques dans les cristaux hémiedres a faces inclinées. *Compt. Rend.* **93**, 1137–1140 (1881)
4. P. Langevin, Précédé et appareil d’émission et de réception des ondes élastiques sous-marines a l’aide des propriétés piézoélectriques du quartz. *Fr. Pat.*, 1918, № 505703
5. W.G. Cady, Piezoelectric resonator. *Proc. Inst. Rad. Eng.* **10**, 83–114 (1922)
6. G.W. Pierce, Piezoelectric oscillators applied to the precision measurement of the velocity of sound in air and CO<sub>2</sub> at high frequencies. *Proc. Amer. Acad.* **60**, 271–302 (1925)
7. S.Ya. Sokolov, Way and the device for test of metals. The copyright certificate USSR, 1928, № 23246 (in Russian)
8. P. Debye, F.W. Sears, On the scattering of light by supersonic waves. *Proc. Nat. Acad. Sci.* **18**(6), 409–414 (1932)
9. R. Lucas, P. Biquard, Nouvelles propriétés optiques des liquides soumis à des ondes ultrasonores. *Compt. Rend.* **194**, 2132–2134 (1932)
10. B. Wool, I. Goldman, Dielectric permeability titanium barium depending on intensity in a variation field. *Rep. Acad. Sci. USSR* **49**(3), 179–182 (1945) (in Russian)
11. B. Wool, I. Goldman, Dielectric permeability titanium metals of 2nd group. *Rep. Acad. Sci. USSR* **46**(4), 154–157 (1945) (in Russian)
12. W.P. Mason, Barium-titanate ceramic as an electromechanical transducer. *Phys. Rev.* **74**(9), 1134 (1948); *Bell. Labor. Rec.* **27**, 285–289 (1949)
13. A. Ananyeva, V. Tsarev, Working out not directed sound detector for ultrasonic frequencies, The Report of Acoustic Laboratory of Physical Institute of Academy of Sciences, 1951 (in Russian)
14. W.P. Mason, *Electromechanical Transducers and Wave Filters*, 2nd edn. (Van Nostrand, Princeton, 1948)
15. W.P. Mason, *Piezoelectric Crystals and Their Applications to Ultrasonics* (Van Nostrand, New York, 1950)
16. L. Bergman, Zur Frage der Eigenschwingungen piezoelektrischer Quarzplatten bei Erregung in der Dickenschwingung. *Ann. d. Phys.* **21**, 553–563 (1935)
17. W. Cady, *Piezoelectricity. An Introduction to the Theory and Applications of Electromechanical Phenomena in Crystals* (Dover, New York, 1946)
18. R.N. Thurston, Effects of electrical and mechanical terminating resistances on loss and bandwidth according to the conventional equivalent circuit of a piezoelectric transducer. *IRE Trans. Ultrason. Eng.* **UE-7**(1), 16–25 (1960)
19. G. Katts (ed.), *Magnetic and Dielectric Devices*, Part 1 (Energiya, Moscow, 1964), p. 416 (in Russian)
20. M. Onoe, H.P. Tiersten, Resonant frequencies of finite piezoelectric ceramic vibrators with electromechanical coupling. *IEEE Trans. Son. Ultrason. Eng.* **10**(1), 32–39 (1963)

21. H.P. Tiersten, Thickness vibrations of piezoelectric plates. *J. Acoust. Soc. Am.* **35**, 53–58 (1963)
22. N. Andreev, Piezoelectric crystals and their application. *Electricity* **2**, 5–13 (1947) (in Russian)
23. N. Andreev, Calculation of the piezoelectric transmitter, Works All-Union Correspondence Power Institute, 1, pp. 5–12 (1951) (in Russian)
24. A.A. Harkevich, *The Theory of Transducers* (Gosenergoizdat, Moscow, 1948) (in Russian)
25. I. Golyamina, To a question about fluctuations by a thickness of the polarised titanium barium plates. *Acous. Mag.* **1**(1), 40–47 (1955)
26. V. Domarkas, R.-J. Kažys, *Piezoelectric Transducers for Measuring Devices* (Mintis, Vilnius, 1974), p. 258 (in Russian)
27. R.-J. Kažys, *Ultrasonic Information Measuring Systems* (Mokslas, Vilnius, 1986), p. 216 (in Russian) I ask to write name Kažys
28. V.V. Malov, *Piezoelectric Resonance Sensors* (Energoizdat, Moscow, 1989), p. 272 (in Russian)
29. A.N. Kutsenko, Matrix sensitivity acoustic strain-measuring device, Works of Scientists OPI. – 1995. – № 1. – C. 122–124 (in Russian)
30. L. Gutin, On the theory of piezoelectric effect. *Mag. Exp. Theor. Phys.* **15**(7), 367–379 (1945) (in Russian)
31. N.A. Shulga, A.M. Bolkisev, *Fluctuations of Piezoelectric Bodies. AS USSR. Mechanics Institute* (Naukova Dumka, Kyiv, 1990), p. 228 (in Russian)
32. V.V. Lavrinenko, *Piezoelectric Transformer* (Energiya, Moscow, 1975), p. 112 (in Russian)
33. I. Glizman, *Piezoceramics* (Energiya, Moscow, 1972), p. 288 (in Russian)
34. S.I. Pugachev (ed.), *Piezoelectric Ceramics Transducers: Reference Book* (Sudostroenie, Leningrad), p. 256 (in Russian)
35. M.V. Korolev, A.E. Karpelson, *Broadband Ultrasonic* (Mashinostroenie, Moscow, 1982), p. 157 (in Russian)
36. A.F. Ulitko, About definition of factor of electromechanical communication in problems of the established fluctuations in piezoelectric ceramics bodies, Materials IX The All-Union Acoustic Conference, Moscow, Acoustic Institute of Academy of Sciences – C. 27–30 (1977) (in Russian)
37. I.G. Minaev, A.I. Trofimov, V.M. Sharapov, On a question about linearization target characteristics piezoelectric force measuring transducers, *Izv. vyzov USSR – “Priborostroenie”*, № 3 (1975) (in Russian)
38. A.I. Trofimov, *Piezoceramic Transducers Static Forces* (Mashinostroenie, Moscow, 1979), p. 95 (in Russian)
39. A.E. Kolesnikov, *Ultrasonic Measurements* (Izdatelstvo Standartov, Moscow, 1982), p. 248 (in Russian)
40. I.N. Ermolov, *The Theory and Practice of Ultrasonic Control* (Mashinostroenie, Moscow, 1981), p. 240 (in Russian)
41. P.G. Dzagupov, A.A. Erofeev, *Piezoelectronic Devices of Computer Facilities, Monitoring Systems and Control* (Politehnika, St. Petersburg, 1994), p. 608 (in Russian)
42. V.M. Pluzhnikov, V.S. Semenov, *Piezoceramic Firm Schemes* (Energiya, Moscow, 1971), p. 168 (in Russian)
43. P. Gribovskiy, *Ceramic Firm Schemes* (Energiya, Moscow, 1971), p. 448 (in Russian)
44. P.G. Pozdnyakov, I.M. Fedotov, V.I. Biryukov, *Quartz Resonators with Film Heaters. The Electronic Technics. Scientifically-techn. The Collection, A Series 9 – Radio Components, Release 4* (Energiya, Moscow, 1971), pp. 27–37 (in Russian)
45. V.M. Sharapov, M.P. Musienko, E.V. Sharapova, in *Piezoelectric Sensors*, ed. by V.M. Sharapov (Technosphaera, Moscow, 2006), p. 632 (in Russian)
46. E.S. Levshina, P.V. Novitskiy, *Electric Measurements of Physical Sizes: (Measuring Transducers). Studies. The Grant for High Schools* (Energoatomizdat, Leningrad, 1983), p. 320 (in Russian)
47. *Electric Measurements of Not Electric Sizes* (Energiya, Moscow, 1975), p. 576 (in Russian)
48. Yaffe B., U. Kuk, G. Yaffe. *Piezoelectric Ceramics* (Mir, Moscow, 1974), p. 288 (in Russian)

49. V. Sharapov et al., The copyright certificate SUN<sup>o</sup> 501306A. Piezoelectric static efforts sensor (in Russian)
50. Firm prospectuses “Bruel and Kjer”, Nerum, Denmark (1995)
51. Firm prospectuses “Kistler Instrumente AG”, Winterthur, Switzerland (1996)
52. Piezoceramic materials. Test methods. Standard of USSR 12370–80, Moscow (1980) (in Russian)
53. Piezoceramic materials. Types and marks. Technical requirements. Standard of USSR 13927–68, Moscow (1968) (in Russian)
54. ELPA, in *Products of Acoustoelectronics and Piezoceramics*, ed. by B.G.M. Parfenov (RIA Delovoy Mir, Zelenograd, 1992), p. 167 (in Russian)
55. V.I. Vinokurov (ed.), *Electric Radio Measurements. The Manual for High Schools* (Visshaya Shkola, Moscow, 1976) (in Russian)
56. O.P. Kramarov, et al., Piezotransducers from metaniobium of lead for ultrasonic resonant thickness gauge. Seminar materials “Radiators and receivers of ultrasonic fluctuations and methods of measurement of acoustic fields”, pp. 27–34 (1966) (in Russian)





<http://www.springer.com/978-3-642-15310-5>

Piezoceramic Sensors

Sharapov, V.

2011, XII, 500 p., Hardcover

ISBN: 978-3-642-15310-5